Journal of Nuclear Materials 465 (2015) 127–134

Contents lists available at ScienceDirect

Journal of Nuclear Materials

journal homepage: www.elsevier.com/locate/jnucmat

Fission product partitioning in aerosol release from simulated spent nuclear fuel

F.G. Di Lemma [a, b, *], J.Y. Colle [a], G. Rasmussen [a], R.J.M. Konings [a, b]

[a] European Commission, Joint Research Centre (JRC), Institute for Transuranium Elements (ITU), Postfach 2340, 76125 Karlsruhe, Germany
[b] Department of Radiation Science and Technology, Faculty of Applied Physics, Delft University of Technology, Delft, 2629JB, The Netherlands

ARTICLE INFO

Article history:
Received 1 December 2014
Received in revised form
28 May 2015
Accepted 1 June 2015
Available online 3 June 2015

Keywords:
Aerosol characterisation
Nuclear aerosol
Fission products
Spent fuel

ABSTRACT

Aerosols created by the vaporization of simulated spent nuclear fuel (simfuel) were produced by laser heating techniques and characterised by a wide range of post-analyses. In particular attention has been focused on determining the fission product behaviour in the aerosols, in order to improve the evaluation of the source term and consequently the risk associated with release from spent fuel sabotage or accidents. Different simulated spent fuels were tested with burn-up up to 8 at. %. The results from the aerosol characterisation were compared with studies of the vaporization process by Knudsen Effusion Mass Spectrometry and thermochemical equilibrium calculations. These studies permit an understanding of the aerosol gaseous precursors and the gaseous reactions taking place during the aerosol formation process.

1. Introduction

Release of radionuclides from nuclear fuel have been extensively investigated for reactor accident scenarios [1–6], however less work has been conducted on release from spent fuel during storage or transport accidents. This topic has acquired interest in view of the Fukushima accident, which has shown the importance of the safety analysis of spent fuel ponds and the possibility of radionuclide release following loss of coolant accidents. Although studies on the safety of spent fuel pools were previously performed, such accidents were believed to be unlikely and no specific measures were considered [7–9]. Following the Fukushima accident new studies have been performed, such as the one of the Nuclear Regulatory Commission [10]. This last study concluded, however, that the spent fuel is only susceptible to a release within a few months after de-fuelling, and that a more favourable loading pattern (avoiding dense packaging) and the improvement of the mitigation strategies could significantly reduce potential releases. Another scenario, which could lead to aerosolization of spent fuel, is related to release during transport of spent fuel casks due to accidents. In this context, a study was performed by Dykes and Machiels [11], which concluded that the probability of such accidents is less than 5×10^{-6}. However, no assessment of the release was performed. Finally even though malicious actions are tried to be ruled out through security measures, it is important to understand the effects of such attacks on spent nuclear fuel. As proposed by Alvarez et al. [12], and demonstrated by the events of September 11th, terrorist attacks are a tangible threat. Magill et al. [13] assessed the consequences for such events but considered a hypothetical respirable fraction for the radionuclide release. Studies on the aerosol release from sabotage events were performed by Molecke et al. [14,15], who performed explosive aerosolization tests using HEDD (High Energy Dispersive Devices) on simulated nuclear reactor rods and analysed the particles released.

The present study aims at describing the aerosol release from spent nuclear fuel under different release scenarios, simulating events in which air contact with overheated spent fuel can occur, such as spent fuel sabotage or accidents during transport or storage. The size distribution is studied as it is needed to evaluate the consequences of a Radiological Dispersion Events (RDE's), for example to assess the extension of the contaminated area. The AED (Aerodynamic Equivalent Diameter) of the particles is the main parameter that can influence the aerosol transport behaviour, but it also determines the probability of deposition of aerosols in the

* Corresponding author. European Commission, Joint Research Centre (JRC), Institute for Transuranium Elements (ITU), Postfach 2340, 76125 Karlsruhe, Germany.
E-mail addresses: fidelma.dilemma@gmail.com (F.G. Di Lemma), jean-yves.colle@ec.europa.eu (J.Y. Colle).

http://dx.doi.org/10.1016/j.jnucmat.2015.06.002

lungs of the exposed population following inhalation. It is thus important to understand the size range in which the high activity radionuclides will be concentrated. Focus is posed in this study on the analysis of the fission product partitioning as function of the particles AED. The ultimate goal is the understanding of the mechanisms influencing the aerosol characteristics. To achieve this, separate effect experiments have been performed analysing different variables (e.g., burn-up, sintering). These results have been finally coupled with studies of the gaseous aerosol precursors. The gaseous release has been obtained from thermochemical equilibrium calculations and experiments using Knudsen Effusion Mass Spectrometry (previously described in Refs. [16,17]). These studies permit understanding the interactions of the gaseous phases during aerosol formation processes.

2. Instrumentation and experimental procedure

The set-up applied in our studies has been described in a recent paper [18]. Laser heating was used in this study to vaporize the samples in air and to generate aerosols that are typical for radioactive release. So far laser heating for simulating accidental scenarios was applied only in a few studies, in relation to reactor power transients [19,20]. Viswanadham et al. [19] studied the effect of laser impulses on UO_2 pellets, while Zanotelli et al. [20] (similar to our application) applied this technique for the production of aerosols and their characterisation. The laser heating technique was chosen in the present experiments for various reasons: limiting interactions between the holder, the heating elements and the sample; avoiding radioactive contamination of the heating components; reaching extreme temperature transients; but especially to have a controlled and reproducible temperature of the sample. This was achieved by applying a PID controller to the laser power, as described in Ref. [18]. In Fig. 1 a comparison of the PID temperature regulation performed for ZrO_2 and UO_2 samples is presented. It can be noticed that the ZrO_2 sample needs a high laser power, prolonged in time, to obtain a quasi-square temperature transients compared to the UO_2 sample. This is related to the higher emissivity of the UO_2 samples with respect to ZrO_2 (respectively ca. 0.85 and 0.6 at the melting point). Difficulties were, however, found while heating the UO_2 samples due to cracking, which influenced the PID regulation causing instability in the control. The cracking of the sample cannot be avoided and is related to a strong thermal shock, due to the low thermal conductivity of UO_2. A custom-made Teflon ring was used to contain the sample and obtain a stable and reproducible heating and vaporization. Once the pellet was correctly heated, aerosols were formed by condensation of the release gases in the cooler air environment and collected for post analyses.

The aerosols produced were analysed applying different techniques (SEM-EDX, Raman spectroscopy, ICP-MS), as described in Ref. [18]. These permit the study of the morphology, the elemental and the chemical composition of the aerosols. Finally, by applying a MOUDI (Micro Orifice Uniform Distribution Impactor) impactor for the collection of the particles, analyses of the size distribution and of the aerosols characteristics as function of their AED size could be performed. The elemental composition was analysed by ICP-MS as function of the particle AED, by washing the aluminium substrates of the various MOUDI impactor stages separately in solution. However experimental difficulties, such as high counts in the blank (for Ba, and Zr) or low counts in the measured solutions (as for La, or Nd), did not permit the quantification of some elements in the different tests. For some of the experiments the trends for Sr, Pd, and Zr could not be clearly observed. This can be related to ejection of inhomogeneous pellets fragments in the first stages with high concentration of these elements, which leads to fluctuation of their

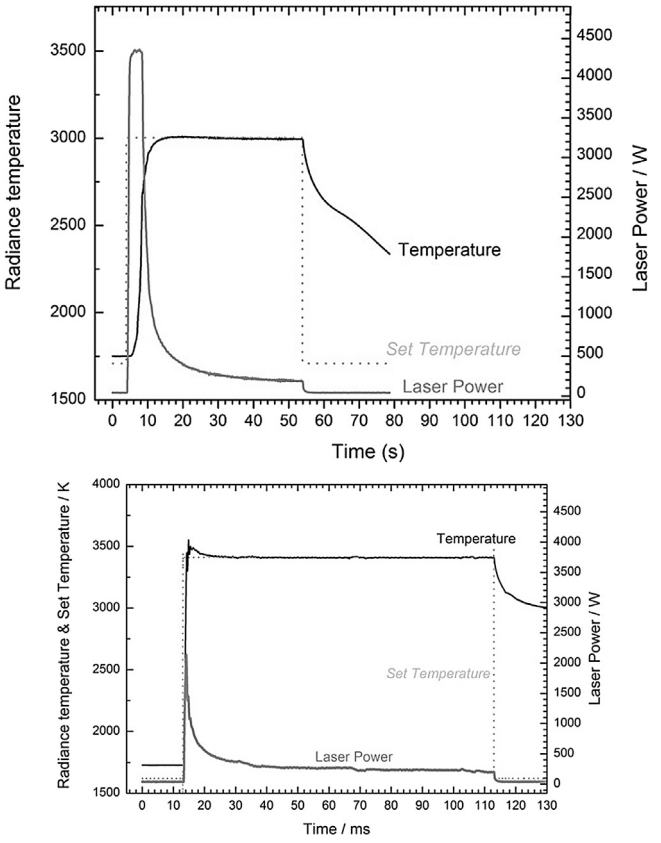

Fig. 1. PID control on temperature for two different samples: Top ZrO_2; Bottom UO_2. Absorbance of UO_2, which, together with a low thermal conductivity, leads to a higher temperature with a lower laser power and shorter time with respect to ZrO_2.

trend through out the stages. The aerosol characterisation was finally coupled with the results from thermochemical equilibrium calculations (performed by Factsage software [21,22]) and KEMS (Knudsen Effusion Mass Spectrometry) experiments. The KEMS was described in Refs. [16,17] and consists of a Knudsen cell coupled with a quadrupole mass spectrometer (with mass range of 1–512 amu). The cell is heated by a tungsten coil, and can be operated in vacuum or with a small flow of different gases (e.g., oxygen, reaching in our experiments a oxygen pressure between 1 and 10 Pa). The molecular beam effusing from the cell is directed and collimated into the ion source of a quadrupole mass spectrometer, in order to detect the gaseous species release as function of the temperature. Calibration of the system was performed by vaporizing, together with the sample, also a known quantity of silver. These vaporization studies permit to identify the gaseous release, and understand the gaseous interactions influencing the aerosol formation.

3. Samples

Different simulated spent nuclear fuel samples were studied. They were composed of a matrix of UO_2 and controlled quantities of non-radioactive isotopes, to simulate the fission products produced in-pile. Simfuels are used to replicate the composition and microstructure of irradiated fuel, and consequently to study the properties and behaviour of spent fuel avoiding the high cost and difficulty of handling such materials. In our experiments different simfuels were used (as summarized in Table 1), applying both in-house made simfuels and simfuels produced by AECL in an industrial-like process. The in-house made samples were obtained by

Table 1
Description of the samples used and of the specific aims of each tested material. The data for the AECL samples were obtained from [23–25].

Sample	Matrix	Fission products	Aim	Description
$SFUO_2$	UO_2	8.58 wt. %	Burn-up effect	Not sintered
$SFUO_2$ 1200	UO_2	8.58 wt. %	Sintering effect	Sintered in furnace at 1200° C in Ar/H_2
AECL 301	UO_2	2.551 wt. %	Burn-up effect	Sintered in furnace at 1650° C
AECL 800	UO_2	7.01 wt. %	Burn-up effect	Sintered in furnace at 1650 °C
UO_2/CeO_2	UO_2	/	Pu behaviour in the aerosols	Different compositions 85/15, 40/60, 60/40 at. %

mixing commercial powders, pressing them by a hydraulic press and then sintering the obtained pellets. During the sintering process the loss of CsI was observed, as confirmed by SEM-EDX and ICP-MS analyses on the samples. CsI loss was observed also when using a rapid sintering method (such as the Spark Plasma Sintering, SPS). Therefore, it was decided to perform first sintering with all the chemical compounds except CsI, which was added after sintering. This was performed by re-grinding the sintered pellet, mixing it with the CsI powder and pressing this mixture in a new pellet. The fission product inventory was calculated by ORIGEN software, and the parameters applied for the calculations are shown in Table 2. This table presents also the chemical compounds used to simulate the different fission products and their relative weight concentrations. Information on the production of the AECL samples can be found in Refs. [23–25]. In these samples the high volatility elements such as Cs, I, and Te are not inserted.

Experiments on inactive samples containing ZrO_2 instead of UO_2 as matrix compound, were also performed, as a first test of the behaviour of compounds with different volatility in a ceramic matrix [18]. Finally for a better evaluation of the behaviour of plutonium in the aerosols separated experiments were performed with mixed samples containing UO_2 and CeO_2. CeO_2 was applied as an inactive ceramic material to simulate PuO_2, due to similar properties [26,27]. These separate effect experiments were performed with mixtures of the powders not pretreated in the furnace, in order to avoid any prior solid solution formation and consequently to know how much material was vaporized from the initial compounds inserted.

Table 2
Composition of the tested materials; the data for the AECL samples were obtained from Ref. [25].

Simfuel samples	$SFUO_2$	AECL 301	AECL 800
Parameters used in Origen			
Enrichment/%	4	none	none
Burn up/at. %	6	3	8
Years in Spent pool	1	0	0

Elements	Chemical form (SF/AECL)	Weight concentration (%)		
U	UO_2	91.42	97.449	92.990
Zr	ZrO_2	0.50	0.336	0.777
Mo	Mo/MoO_3	0.45	0.356	0.980
Pd	Pd/PdO	0.21	0.147	0.652
Ba	$BaO/BaCO_3$	0.23	0.150	0.433
Y	Y_2O_3		0.040	0.075
Sr	SrO	1.38	0.223	0.531
Ce,Pu	CeO_2	4.51	0.304	0.717
La,Am,Cm	La_2O_3	0.38	0.113	0.367
Ru,Tc	Ru/RuO_3	0.33	0.360	1.026
Rh	Rh_2O_3		0.028	0.038
Nd,Pm,Sm	Nd_2O_3	included in La_2O_3	0.494	1.418
I	CsI	0.07		
Cs	Cs_2 ZrO_3	0.53		

4. Post-analyses

4.1. Aerosol characterisation

Similar aerosol features were found for all the samples tested. No differences in the aerosol characteristics were observed between ZrO_2 samples, UO_2 compacted powders and industrial-like UO_2 pellets either. The aerosols had a bimodal size distribution (an example of which is shown in Fig. 2) and can be divided in two classes: big spherical micrometer particles or fragments, which were collected as a first peak in the bigger AED size range (AED $\geq$ 10 μm), and smaller agglomerates of submicron particles, corresponding to the second peak in the nanometric AED size range (as shown in Fig. 3). These two different morphologies are related to different formation processes [18,28,29]. The bigger particles are formed by the ejection of liquid particles from the melted layer or solid material from the pellet, due to the mechanical shock caused by the laser heating. The nanometric particles are instead formed from the condensation of the vaporized material. These particles then agglomerate in complicated structures due to the high number of primary particles formed.

An important outcome of the post-analyses was the observation that the "fission product" concentration varies with the particle size. This was observed by SEM-EDX as function of the geometrical particle size, when the particles were collected with filters and as function of the AED when the particles were collected by the MOUDI impactor. In particular a higher concentration of the high volatile compounds was found in the smaller size particles with respect to the bigger size. The bigger aerosols were instead enriched in the low volatile elements such as the matrix elements (Zr or U) and also Ba and Ce. A similar trend has been observed in experiments over a molten corium pool simulating FP releases during in-vessel severe accident sequences, such as the COLIMA

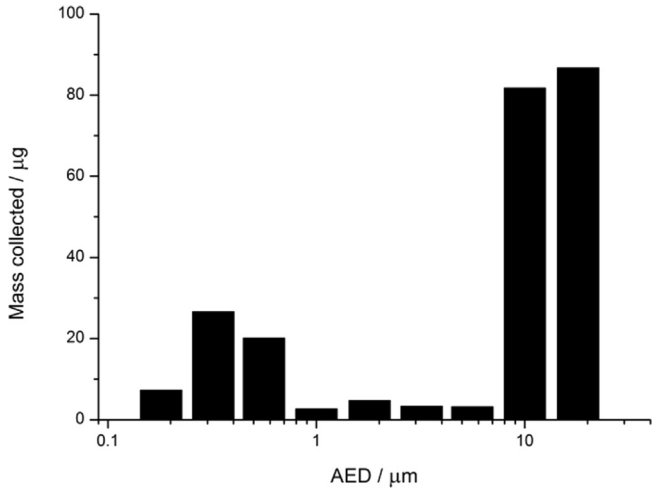

Fig. 2. Example of a size distribution for the tested simfuels obtained from the ICP-MS analysis, showing a bimodal size distribution.

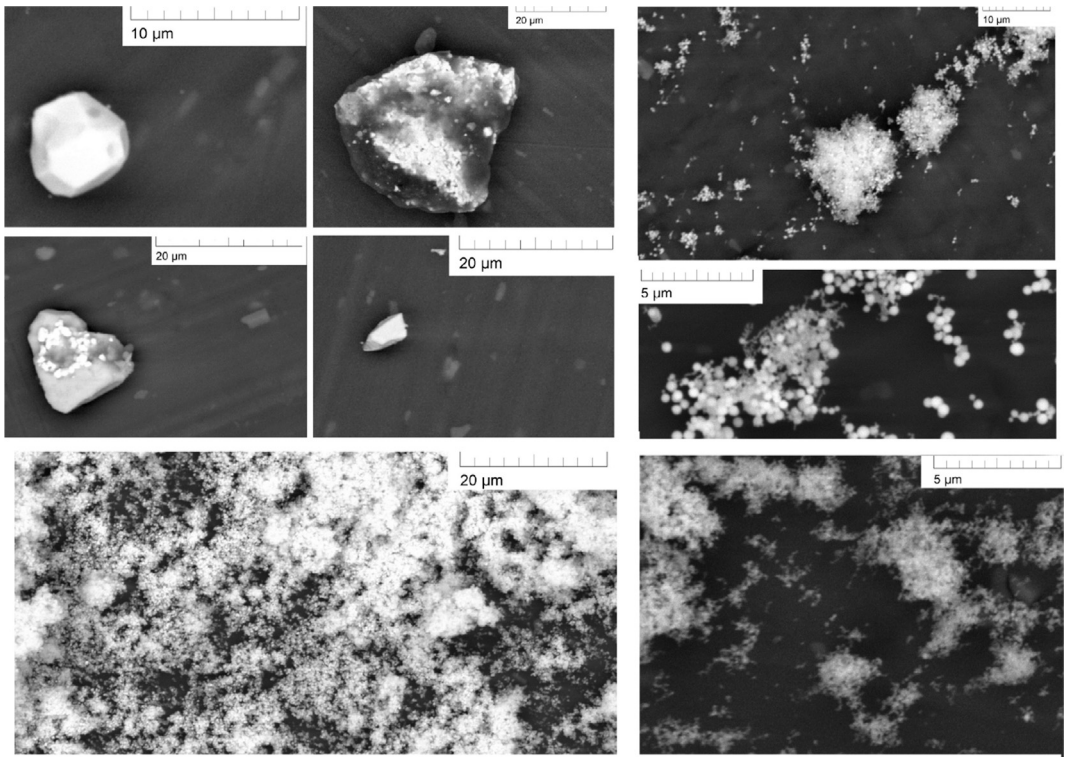

Fig. 3. The aerosols collected for the simfuel (sample AECL 800). A similar morphology was observed for all the samples tested.

CAU3 test [30]. This partitioning can be related to the aerosol formation mechanism [18]. The bigger particles formed by the ejection of the melted layer or solid fragments will be enriched in the matrix and the low volatile elements, which are retained in the pellet. While the smaller particles, formed by the condensation of the vapour, will be enriched in the higher volatile elements [18,28,29]. In all the particles mainly U was observed. Cs and I were usually detectable in the smaller AED together in a ratio Cs/I of 1 for both $SFUO_2$ and ZrO_2 samples. Moreover also Cs without I was detected for the $SFUO_2$ sample. Two different sources were identified for the Cs release of this sample: Cs released from CsI and from Cs_2 MO_x (M = Metal, such as Zr, Mo, etc). This second Cs release could come from the separate vaporization of Cs_2 ZrO_3, as CsO and ZrO_2 [31] as this compound was inserted in the simulated fuel, or could be related to the formation of Cs_2 MoO_4 as predicted from the thermochemical calculations. In fact another element detected in the smaller particles was Mo, although it was difficult to determine its chemical form (Cs_2 MoO_4 or MoO_3). Finally the different "fission product" concentrations between the samples (corresponding to 3, 6 and 8 at.%) did not influence the aerosols characteristics.

The "fission product" elemental partitioning with AED size was also confirmed by the ICP-MS analyses of the solutions obtained from washing separately each impactor stage, as described in Ref. [18]. From these analyses different trends were observed for the different simulated fission products. The results from all experiments (as shown in Fig. 4) can be summarized as follows:

- U, Ce, Zr, Y, La, Nd showed a similar trend, diminishing from the bigger to the smaller AED.
- The Ba concentration was quite stable throughout the stages, but it should be realised that the Ba is difficult to measure by ICP-MS due to the contamination from the environment.
- The more volatile fission products such as Cs but also Ru and Mo were enriched instead in the smaller AED (as shown in Fig. 5). The high volatilization of these metallic fission products, which are generally thought to be retained in the pellet, is related to the oxidising conditions applied in our experiments. This will lead to the formation of Ru and Mo oxides, which have a higher volatility than the metals.
- It is finally worth noticing that the behaviour for Pd and Rh was observed to be comparable in the experiments with the AECL simfuel. The elements are usually considered in the middle class volatile elements. Their concentration was observed to increase with decreasing AED, reaching a peak in Stage 6/7 (Cut off sizes AED 0.56–0.32 μm) and decreasing again in stage 8 (AED 0.18 μm).

The pellets were also analysed by SEM/EDX as this can give important information on the vaporization process. Comparing the

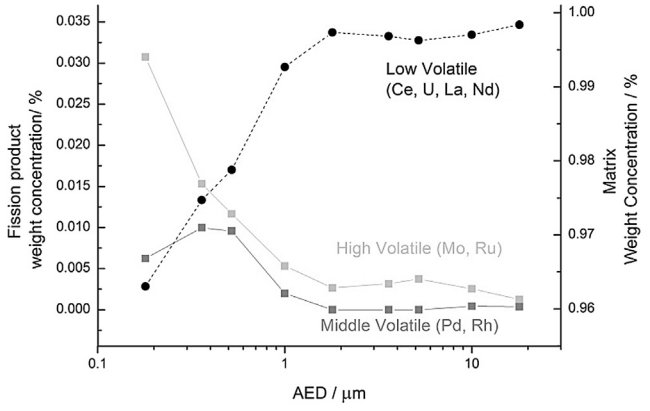

Fig. 4. Concentration trends for the elements in the different volatile class in the aerosols, as function of the AED, for the AECL simfuels as obtained by ICP-MS analysis.

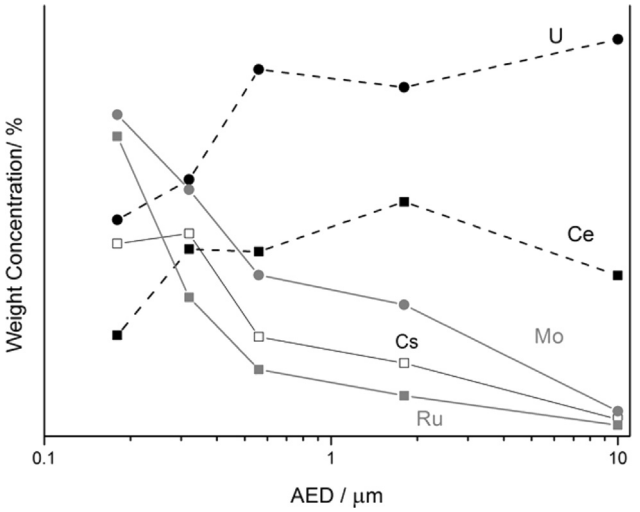

Fig. 5. Concentration trends for the matrix elements and high volatile class elements, as function of the AED of the aerosols. The absolute proportion between the elements is not reproduced in order to present clearly the trends, which show clearly the relation with the different release and aerosol formation processes.

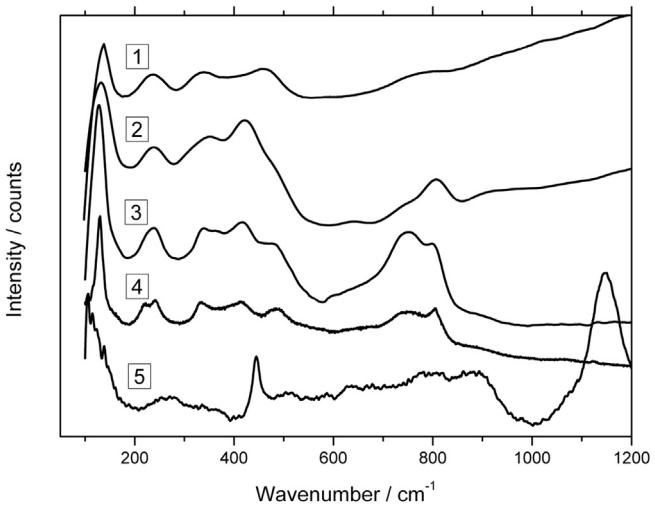

Fig. 6. Comparison of the RAMAN patterns of the aerosols collected and standards measured. The spectra from the aerosols collected from $SFUO_2$ simfuel are shown in line (1,2), while aerosols from stoichiometric UO_2 are shown in spectrum (3). It can be noticed for the $SFUO_2$ simfuel that the composition of the aerosols collected is UO_{2+x} (and not U_3O_8) possibly due to competing oxidative processes with the fission products, while for UO_2 the aerosols are made of U_3O_8. Spectrum (4) shows the standard spectrum of U_3O_8; while (5) the spectrum for a standard of UO_2.

melted and unmelted region confirmed the ICP-MS results. It was observed that the low volatile elements (such as Ba, La, Ce) were retained in the pellet after the laser pulse, while CsI and the metallic (Ru, Mo) elements were depleted confirming their vaporization. These metals compounds were found before the laser heating experiments in the pellet as metal alloy precipitates (containing Ru, Mo, Pd) due to their insolubility in the matrix [23,32].

Finally to test if a different size partitioning could occur in the aerosols between U and Pu, some experiments were performed with UO_2 and CeO_2 powder mixtures with different concentrations (85/15, 40/60, 60/40 at. %). From all these experiments it was observed that the main vaporized specie was UO_x. This effect was confirmed by the analysis of the pellet in the melted area, which showed that this area was enriched in Ce. The content of Ce was found to be small in the smaller AED, its concentration increasing in the particles with bigger AED. This again demonstrates that the different volatility of the compounds has a strong effect on their partitioning with aerosol size.

The Raman spectroscopy analyses of the aerosols did not permit the identification of the fission product phases, as these have a low concentration. This demonstrates the importance of applying different techniques in analysing the aerosols, because SEM-EDX and ICP-MS permitted detecting low elemental concentrations in the aerosols and their trends. On the other hand, the oxidation state of uranium in the aerosol was detected by Raman spectroscopy. Raman spectroscopy showed that the aerosols released from the UO_2 pellets were clearly oxidized to U_3O_8 in all the analysed stages (as shown in Fig. 6), based on a comparison with literature data [33–35] and standards measured in our laboratory. This phase was also observed for the mixed sample with UO_2/CeO_2, in which the main compound released was U_3O_8 and CeO_2 was retained in the pellet. The effect of sintering of the UO_2 pellets on the Raman spectra of the aerosols was also examined. However when performing the sintering in reducing conditions (Ar/H_2 environment) the starting pellet material was UO_{2-x}. This seems to have an effect on the aerosols oxidation state as the results showed the formation of UO_{2+x}. Kinetic effects may have limited the oxidative process, reducing the gaseous release of UO_3 and the formation of the solid phase of U_3O_8. It was also observed that for the simfuels ($SFUO_2$) the presence of the fission products has an effect on the Raman spectra of the aerosols. They showed the characteristics spectra of UO_{2+x} and not U_3O_8, even when the pellet was not sintered. Fission products, such as Mo, could have affected the oxidation of the pellet and decreased the release of UO_3 due to a competing oxidation process. This effect was confirmed by comparing the results with the Raman spectra from the AECL samples, in which Mo was inserted already in the oxide form. In this case the aerosols presented just the U_3O_8 Raman peaks.

4.2. Equilibrium vaporization studies

KEMS measurements and thermochemical equilibrium calculations were performed to understand the gaseous aerosol precursors and chemical interaction occurring in the gaseous phase under equilibrium conditions. The KEMS experiments were conducted in vacuum and under a constant O_2 flow. The thermochemical equilibrium calculations were performed with a constant pressure (1×10^5 Pa), one case with the O_2 fixed activity to 0.21×10^5 Pa simulating the vaporization process in air environment (as in our laser heating experiments), and the other in absence of O_2 in the environment, the oxygen potential being thus imposed by the release from the simfuel. The choice of using a fixed pressure calculations was explained in Ref. [36] and showed good agreement with the experimental observations. This choice is consistent with the conditions in the system as a small amount of material is vaporized in a comparatively very large vessel kept at constant pressure and air environment. Thus the gases are free to expand in the cell environment.

The KEMS experiments revealed similar release patterns for all the samples. At low temperature (900–1200 K) gaseous release of I and Cs was detected, followed by the gaseous release of Pd, Ba and Sr (as shown in Fig. 7). Finally the low volatile species such as U, Ce, La, Nd, and Zr were detected at high temperature. Cesium was detected as Cs^+ ion, which is the product of the fragmentation and ionisation of molecular species at the electron energy applied. The peak at the lowest temperature was assigned to gaseous CsI because of its congruent signal with the CsI^+ and I^+ ion signals. In some cases a second release was observed for Cs around 1100 K in the $SFUO_2$ experiment (as shown in Fig. 7), which was not observed

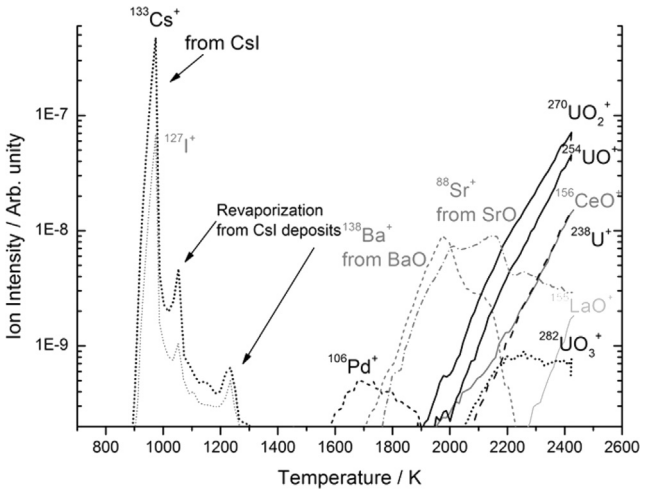

Fig. 7. An example of the KEMS results for simfuel, showing the high volatile elements and lower volatile compounds released in vacuum conditions.

for the I^+ signal. This can be related to the vaporization of Cs_2 ZrO_3, which was added to the $SFUO_2$ sample, and which vaporizes incongruently to CsO and ZrO_2 [31]. Alternatively it could originate from Cs_2 MoO_4, which vaporises congruently [37], as this compound was predicted to be stable by the thermochemical equilibrium calculations, also with no O_2 excess. This confirms the SEM-EDX observations of the aerosols that suggest a second source for the Cs release than CsI. Moreover by the KEMS experiments and the thermochemical calculations we could deduce the chemical form of the released gases Pd as metal, Sr and Ba and also the Lanthanides and the Actinides as oxides.

The influence of an oxidising environment was studied also in the KEMS experiments (by a O_2 flow in the cell). The most obvious difference with the experiments in vacuum was the release of MoO_3, and the lower temperature release of UO_x species. No substantial differences were observed for the other elements, including ruthenium. Evidently the oxygen potential imposed by the oxygen flow was too low for oxidation to gaseous RuO_x species to occur. This different behaviour between Mo and Ru was already observed in previous KEMS experiments on CsI–Ru and CsI–Mo mixtures [36], which showed that gaseous MoO_3 was formed while no gaseous Ru species were detected. The release of the metallic fission products in oxidative conditions was predicted also by the thermochemical equilibrium calculations. Moreover in presence of O_2 the thermochemical calculations showed that for the $SFUO_2$ sample the presence of Mo can give rise to release of free I_2 by the breaking the CsI bond, as a results of the formation of Cs_2 MoO_4, as also observed in our separate effect experiments [36].

5. Discussion

In this work the aerosols release from spent nuclear fuel was simulated with the aim of understanding the fission product partitioning as a function of aerosol size (AED). The principal issue was whether the highly active radioisotopes can be concentrated in the small particles, as this influences the risk evaluation for the population because these particles can be transported over long distances and penetrate deep in the lungs if inhaled.

In the tests indeed a size partitioning of the elements as function of their AED size was observed. For all the tested samples it was observed that the highly volatile fission products are enriched in the smaller particle fractions, while the non-volatile elements are concentrated in the bigger particles (first impactor stages with bigger AED>1 μm). This effect can be related to the aerosol formation mechanism. The smaller particles are formed by the rapid condensation of the vapour and are thus concentrated in the high volatile elements. The larger particles are created by ejection of liquid or solid material from the pellet, and are thus enriched in the low volatile elements retained in the matrix. The size partitioning trends observed can be summarized as follows:

- U containing aerosols were found in all AED size fractions as the main constituent of all aerosols, which is not surprising as it is constituting at least 91 wt. % of the sample. Raman spectroscopy showed that the chemical form of the uranium aerosols is U_3 O_8 or UO_{2+x}.
- Cs was observed in the smaller particles (high volatile element trend). It was generally detected together with I in a ratio of approximately 1, as it was insert as CsI in the simfuel. However, a second source for Cs release was observed as SEM-EDX analysis showed aerosols containing Cs but no I. Thermochemical equilibrium calculations predicted the possibility of separated gaseous release of Cs and I due to reaction with Mo to form a new compound, Cs_2 MoO_4. Alternatively, the second release could be related to the vaporization of Cs_2 ZrO_3, as CsO and ZrO_2.
- Ru and Mo, which are present in the fuel in the metallic form, were released in the aerosolization experiments in air. ICP-MS measurements indicated that they are concentrated in the smaller aerosol fraction and that partitioning follows the trend of high volatile elements such as Cs. This is related to the increase volatility due to the formation of gaseous oxides in an air environment. Their release could not be observed in the KEMS in vacuum condition, while Mo but not Ru volatilisation was observed in the KEMS experiments with O_2 flow.
- The Pd concentration showed an increase with decreasing particles size, reaching a maximum and then decreasing again in stage 8 (AED < 180 nm). A similar size distribution was also observed for Rh, as they are assigned to the same volatility class. Pd was released in the metallic form, as predicted by the thermochemical equilibrium calculations.
- Ce was enriched in the bigger particles which shows that it is preferentially retained in the matrix. From separate effect studies simulating the behaviour of Pu in the aerosols by a (U,Ce) O_2 matrix, a size partitioning between the two elements was observed. Ce was concentrated in the bigger size ranges with respect to U, which was the main phase (in the form of U_3 O_8) in the smaller AED particles.
- Nd, La, Sr, Y, Zr, and Ba were difficult to evaluate due to their low concentration in the aerosols or due to contamination by the environment and/or precedent tests. By coupling the results from different experiments it was possible to assess their behaviour. They showed the trend of the low volatile element class (or matrix elements); their concentration decreases with smaller particles size. Thermochemical equilibrium studies and KEMS experiments indicates that they were present as oxide species.

Molecke et al. [15] studied the fission product enrichment in the aerosols and their respirable size fraction. They performed explosive aerosolization tests on simulated spent nuclear rods, composed of a zircalloy cladding and simulated spent nuclear fuel pellets. However their simulated spent fuels contained only a limited number of fission products (CsI, RuO_2, SrO, Eu_2 O_3), which were chosen as representative for the different fission products volatile classes. They concluded that Cs was enriched in the respirable fraction, similar to the results of this study. They concluded that the hypothesis of 5% aerosolization in the respirable fraction for spent fuel obtained in calculations by Luna et al. [38] was

conservative, as they found that <2% of U was found in the respirable fraction. A higher concentration of the particles in the respirable fraction was observed in the present work, due to the impossibility with the laser impact set-up to perform a scaled explosive fragmentation of the sample. On the other hand the current study provided a more complete investigation of the behaviour of the different fission products in the aerosols, analysing both the particles and the gaseous release by separate experiments and calculations, thus providing a better understanding of the vaporization process and of the chemical reactions taking place and of their influence on the aerosol characteristics.

Finally the difference between simfuel and irradiated fuel and its effect on our observations needs to be discussed. The main distinction is related to the differences in the microstructure of the fuel. In the simfuels the added fission products are predominantly present at the grain boundaries, with the exception of the elements that can dissolve in the UO_2 matrix under equilibrium conditions, such as Zr and the rare earths. Release from simfuel thus takes predominantly places via the high diffusivity grain boundary network. In irradiated fuel, a significant fraction is, however, present in the fuel grains, as atoms dissolved in defects, defects clusters, voids or gas inclusions. Release and vaporisation from irradiated fuel is thus more complex, involving also slow diffusion of atoms and gas inclusions in the fuel matrix, and the enhancement of grain boundary diffusion due to the accumulation of fission gas bubbles at these sites. Comparison with the KEMS experiments on irradiated fuel in vacuum [39] shows that in that material the release takes place in much broader temperature ranges, the maximum release peak appearing generally at higher temperature (for CsI >1200 K). Hiernaut et al. [39] also studied oxidising conditions, which revealed a shift of the release to lower temperature which was caused by the oxidation of the uranium dioxide matrix, but also in this condition the release of volatile elements continues up to high temperatures. Thus the use of simfuel instead of irradiated fuel will mainly affect the quantities of the fission products released into the gas phase, but not significantly the aerosol formation processes from the gaseous phase.

6. Conclusions

This study has shown the importance of coupling different techniques for the evaluation of the release of aerosols from spent fuel, here simulated by different simfuels. The equilibrium vaporization studies provide information on the release behaviour and on the gaseous precursors of the aerosols. In particular these techniques were able to predict the chemical forms of the aerosols, the influence of different environments on the release and to understand the chemical reactions that lead to the formation of new compounds. The laser aerosolization experiments provide the possibility of studying the effect of kinetics, due to the rapidity of our experiments, and the aerosol characteristics (such as the size distribution, the morphology, the elemental partitioning with size, and the chemical composition of the main released phase). A good agreement was obtained between the predicted gaseous aerosol precursors and the aerosols in this study. Finally the importance of separate effect experiments should be stressed, as they complement the irradiated nuclear fuel release studies, and help to obtain a better understanding of the aerosol formation mechanisms and of the gaseous release processes (e.g., different sources for the gaseous release, chemical reactions, etc.).

From these experiments it can be concluded that oxidising conditions for the aerosolization experiments, simulating scenarios in which overheated fuel is in contact with air, will lead to the release of not only the volatiles Cs and I but also of the metallic fission products Ru and Mo. These will concentrate in the smaller AED particles size, together with CsI. This effect can have a high influence on the risk associated with the inhalation of aerosols released from spent fuel, as these elements are highly radio-toxic. Moreover, the thermochemical equilibrium calculations showed an important effect of the release of the metallic fission products, as they can influence the release of free molecular iodine (this was further demonstrated in the separate effect study in Ref. [36]). On the other hand, it was observed that Pu, for which a high health risk is associated with its incorporation by inhalation, will be concentrated in the particles with bigger AED. It was found that the uranium chemical form in the aerosols is U_3O_8 and/or UO_{2+x}. These chemical compounds are classified in the low soluble class, but their solubility is higher with respect to the starting material UO_2 [40]. Moreover the small dimension of these particles (AED < 0.18 μm), will lead to faster dissolution kinetics [41]. Thus these particles will constitute a high risk for the population.

Finally this study has demonstrated that a partitioning of the different (radioactive) elements takes place as function of the AED in the aerosols released from spent nuclear fuel. This is an important observation to consider in simulation codes for Radioactive Dispersion Events (such as ARGOS [42], RODOS [43], HOTSPOT [44]). Currently these codes consider as input the total activity of the source and the quantity dispersed in the respirable fraction, and calculate from these data a homogeneous distribution of the source activity over the different size ranges. From this assumption the extension and radioactivity level of the contaminated area are calculated. The results from the present study showed the partitioning of the fission products as function of particles size, and thus demonstrate the need of implementing a non-homogeneous element-specific activity distribution as input for these codes when analysing spent fuel accidents.

Acknowledgements

F.G.D. would like to acknowledge the constructive contribution to this work: O. Beneš, B. Cremer, M. Ernstberger, M.A. Hernandez Ceballos, K. Mayer, V. Rondinella, M. Sierig, J. Somers, D. Staicu, V. Typleck. This work is supported by the 7th Framework Program of the European Commission.

References

[1] H.J. Allelein, A. Auvinen, J. Ball, S. Gúntay, L.E. Herranz, A. Hidaka, A.V. Jones, M. Kissane, D. Powers, G. Weber, State of the Art Report on Nuclear Aerosols, Tech. Rep. NEA/CSNI/R(2009)5, OECD, Nuclear Energy Agency, 2009.
[2] F.C. Iglesias, B.J. Lewis, P.J. Reid, P. Elder, J. Nucl. Mater. 270 (1999) 21–38.
[3] M.P. Kissane, Nucl. Eng. Des. 238 (2008) 2792–2800.
[4] W. Krischer, M.C. Rubinsten, The Phebus Fission Product Project, first edn., Elsevier applied science, 1992.
[5] L.E. Herranz, J. Ball, A. Auvinen, D. Bottomley, A. Dehbi, C. Housiadas, P. Piluso, V. Layly, F. Parozzi, M. Reeks, Prog. Nucl. Energy 52 (2010) 120–127.
[6] P. Bottomley, B. Clément, T. Haste, D. Jacquemain, M. Powers, D.A. Schwarz, B. Teisseire, R. Zeyen, Ann. Nucl. Energy 61 (2013) 1–230.
[7] A. Barto, Y.J. Chang, K. Compton, H. Esmaili, D. Helton, A. Murphy, A. Nosek, J. Pires, F. Schofer, B. Wagner, Consequence Study of a Beyond-design-basis Earthquake Affecting the Spent Fuel Pool for a U.S. Mark I Boiling Water Reactor, Tech. Rep. NUREG-2161, Office of Nuclear Regulatory Research, US Nuclear Regulatory Commission, 2014.
[8] T.E. Collins, G. Hubbard, Technical Study of Spent Fuel Pool Accident Risk at Decommissioning Nuclear Power Plants, Tech. Rep. NUREG-1738, U.S. Nuclear Regulatory Commission (NRC), 2001.
[9] IAEA Nuclear Fuel cycle and material section, Health and Environmental Aspects of Nuclear Fuel Cycle Facilities, Tech. Rep. IAEA-TECDOC-918, International Atomic Energy Agency (IAEA), 1996.
[10] H. Esmaili, vol., in: Proceeding of the National Academy of Science (NAS), Presentation of the Office of Nuclear Regulatory Research (NRC), 2014.
[11] A. Dykes, A. Machiels, Packaging, Transport, Storage & Security of Radioactive Material, Radioact. Mater. 21 (2010) 51–61.
[12] R. Alvarez, J. Beyea, K. Janberg, J. Kang, E. Lyman, A. Macfarlane, G. Thompson, F.N. von Hippel, Sci. Glob. Secur. 11 (2003) 1–51.
[13] J. Magill, D. Hamilton, K. L'utzenkirchen, M. Tufan, G. Tamborini, W. Wagner, V. Berthou, A. von Zweidorf, Sci. Glob. Secur. 15 (2007) 107–132.

[14] M.A. Molecke, J. Brockmann, D. Lucero, M. Steyskal, M.W. Gregson, vol. SAND2006–5556C, Paper 116, in: Proceedings of the 47th Annual Meeting of the INMM, 2006.
[15] M.A. Molecke, J.E. Brockmann, L.A. Klennert, M. Steyskal, M.W. Gregson, W. Koch, O. Nolte, W. Br'ucher, G.G. Pretzsch, B.A. Autrusson, O. Loiseau, Packaging, Transport, Storage & Security of Radioactive Material, Radioact. Mater. 19 (2008) 95–101.
[16] J.P. Hiernaut, J.Y. Colle, R. Pflieger-Cuvellier, J. Jonnet, J. Somers, C. Ronchi, J. Nucl. Mater. 344 (2005) 246–253.
[17] J.-P. Hiernaut, P. Gotcu, J.-Y. Colle, R.J.M. Konings, J. Nucl. Mater. 378 (2008a) 349–357.
[18] F.G. Di Lemma, J.Y. Colle, R.J.M. Konings, J. Aerosol Sci. 70 (2014) 36–49.
[19] C.S. Viswanadham, K.C. Sahoo, T.R.G. Kutty, K.B. Khan, V.P. Jathar, S. Anantharaman, A. Kumar, G.K. Dey, Pramana J. Phys. 75 (2010) 1267–1272.
[20] W.A. Zanotelli, G.D. Miller, E.W. Johnson, Aerosol Characterization from a Simulated HCDA : 1979, Annual Report, NUREG/CR-2109, MLM-2790–R7, 1981.
[21] C.W. Bale, P. Chartrand, S.A. Degterov, G. Eriksson, K. Hack, R.B. Mahfoud, J. Melancon, A.D. Pelton, S. Petersen, Calphad 26 (2002) 189–228.
[22] C.W. Bale, E. Bélisle, P. Chartrand, S.A. Decterov, A. Eriksson, K. Hack, I.H. Jung, Y.B. Kang, J. Melancon, A.D. Pelton, C. Robelin, S. Petersen, Calphad 33 (2009) 295–311.
[23] P.G. Lucuta, B.J. Palmer, H. Matzke, D.S. Hartwig, in: Proceedings of Second International Conference on CANDU Fuel, 1989, pp. 132–146.
[24] P.G. Lucuta, R.A. Verrall, H. Matzke, B.J. Palmer, J. Nucl. Mater. 178 (1996) 48–60.
[25] V.V. Rondinella, H. Matzke, J. Nucl. Mater. 238 (1996) 44–57.
[26] H.S. Kim, C.H. Joung, B.H. Lee, J.Y. Oh, Y.H. Koo, P. Heimgartner, J. Nucl. Mater. 378 (2008) 98–104.
[27] A.K. Tyagi, B.R. Ambekar, M.D. Mathews, J. Alloys Compd. 337 (2002) 277–281.
[28] S.D. Lee, E.G. Snyder, R. Willis, R. Fischer, D. Gates-Anderson, M. Sutton, B. Viani, J. Drake, J. MacKinney, J. Hazard. Mater. 176 (2010) 56–63.
[29] F.T. Harper, S.V. Musolino, W.B. Wente, Health Phys. 93 (2007) 1–16.
[30] P. Piluso, E. Boccaccio, J.M. Bonnet, C. Journeau, P. Fouquart, D. Magallon, I. Ivanov, I. Mladenov, S. Kalchev, P. Grudev, M. Leskovar, H. Alsmeyer, vol. Paper 79, in: Proceedings of the International Conference Energy New Europe, 2005.
[31] M. Ali Basu, R. Mishra, S. Bharadwaja, A.S. Kerkara, K.N.G. Kaimala, S.C. Kumarb, D. Das, J. Alloys Compd. 314 (2001) 96–98.
[32] T. Muromura, T. Adachi, H. Takeishi, Z. Yoshida, T. Yamamoto, K. Ueno, J. Nucl. Mater. 151 (1988) 327–333.
[33] G.C. Allen, I.S. Butler, N. Anh-Tuan, J. Nucl. Mater. 144 (1987) 17–19.
[34] D. Manara, B. Renker, J. Nucl. Mater. 321 (2003) 233–237.
[35] C. Jegou, R. Caraballo, S. Peuget, D. Roudil, L. Desgranges, M. Magnin, J. Nucl. Mater. 405 (2010) 235–243.
[36] F. G. Di Lemma, J. Y. Colle, O. Beneš, R. J. M. Konings, Accepted for publication in J. Nucl. Mater.
[37] M. Yamawaki, T. Oka, M. Yasumoto, H. Sakurai, J. Nucl. Mater. 201 (1993) 257–260.
[38] R.E. Luna, K.S. Nuehasuser, M.G. Vigil, Project Source Terms for Potential Sabotage Events Related to Spent Fuel Shipments, Tech. Rep. SAND99–0963, Sandia National Laboratories, 1999.
[39] J.-P. Hiernaut, T. Wiss, D. Papaioannou, R.J.M. Konings, V.V. Rondinella, J. Nucl. Mater. 372 (2008b) 215–225.
[40] A.F. Eidson, J. Health Phys. 67 (1994) 1–14.
[41] J.R. Cooper, G.N. Stradling, H. Smith, S.E. Ham, Int. J. Radiat. Biol. Relat. Stud. Phys. Chem. Med. 41 (1982) 421–433.
[42] ARGOS, Computer Software CBRN Whitepaper. Decision Support for Emergency Management, 2008 accessed from: www.pdc.dk/Argos/downloads/ARGOS_whitepaper.pdf.
[43] RODOS, RODOS: Decision Support System for Off-site Nuclear Emergency Management in Europe, 2000 accessed from: http://www.rodos.fzk.de/Overview/moreinfo.html.
[44] HotSpot, NARAC: HotSpot 2.07.2, Computer Software, 2011 accessed from: https://narac.llnl.gov/HotSpot/HotSpot.html.